



HETEROLEPTIC METAL(II) COMPLEXES OF CURCUMIN AND 2,2'-BIPYRIDINE: SYNTHESIS, CHARACTERIZATION, MOLECULAR MODELING AND PRELIMINARY ANTIMICROBIAL INVESTIGATION

Shyam LAL,^a Mukesh Chandra JOSHI^b, Sunita HOODA^a and Vikrant KUMAR^{a*}

^a Department of Chemistry, Acharya Narendra Dev College (University of Delhi), Kalka Ji, New Delhi-110019, India

^b Department of Chemistry, Motilal Nehru College, University of Delhi, Delhi-110021, India

Received September 18, 2017

Three mononuclear metal complexes [(curcu)M(bpy)]Cl **1-3** of nickel^{II} (**1**), copper^{II} (**2**) and zinc^{II} (**3**) derived from curcumin (curcu) and 2,2'-bipyridine (bpy) have been isolated and characterized by analytical and spectral methods, *viz.* elemental analyses, molar conductance, magnetic susceptibility measurements, mass spectrometry, IR, UV-visible spectrometry and molecular modeling studies. IR spectral frequencies exhibited curcumin and 2,2'-bipyridine both behave as bidentate ligand and coordinate to metal ion through the carbonyl oxygen and nitrogen atoms respectively. All the complexes showed molar conductance corresponding to 1:1 electrolytic nature. Ni^{II} and Cu^{II} complexes were confirmed possessing square planar geometry however Zn^{II}, tetrahedral. Metal complexes along with curcumin and 2,2'-bipyridine were examined against the opportunistic pathogens. The results obtained indicate that metal complexes have reasonable antimicrobial potential.



INTRODUCTION

Naturally occurring phenolic pigment, Curcumin; chemically, [1,7-bis(4-hydroxyl-3-methoxyphenyl)-1,6-heptadiene-3,5-dione] is a major component of the *Curcuma longa* Linn,¹ which is commonly used as a yellow coloring and flavoring agent in foods. Recent studies have shown that curcumin possesses a specific property of binding to metals and as a multipotent agent for combating to potent biological as well as pharmacological activities.²⁻⁸ Thus, for the past decade curcumin as a ligand has been the subject of great interest in modern coordination chemistry.⁹⁻¹² Curcumin has a specific chemical motif, a bis- α,β -unsaturated- β -diketone which exhibits keto-enol tautomerism (**Figure 1**). The virtue of coordination property of curcumin leads to tailoring a rational drug design including a number of metal complexes and

scavenge the active free-radicals which makes it a more potent bioactive agent *viz.* as antimicrobial agent, anticarcinogenic, antialzheimer, used in catalysis, radiodiagnostic and several other applications.¹³⁻¹⁷ Research analysis postulates that the biological properties of curcumin are significantly enhanced upon coordination with metal ion.¹⁸⁻¹⁹ On the other hand, heterocyclic compounds such as pyridine, phenanthroline, bipyridine, and their respective derivatives etc. have been shown extended biological activities when coordinated with metal ion.²⁰⁻²¹ Various enzymes, vitamins, proteins and other life regulating biomolecules, most of which consist of N- and/or O- containing heteroatoms which are the key of chelation with transition metal ions.

Thus, specific biological and pharmacological role of curcumin, bipyridine and various role of transition metal ions in daily life, could have made

* Correspondence author: Tel.: +91-11-26294542; Fax: +91-11-26294540.
E-mail address: vikrantkumar@andc.du.ac.in (Vikrant Kumar)

them as more medicinal pharmacophore with low toxicity and low side effects.²²⁻²⁴ Attention in our present endeavor has been given to preparation, structural elucidation and antimicrobial activity of three heteroleptic complexes with Ni^{II}, Cu^{II} and Zn^{II} metal ions bearing curcu/bpy mixed ligand.

RESULTS AND DISCUSSION

Complexes (**1-3**) were obtained during the reaction of metal^{II} chloride (M^{II} = Ni, Cu and Zn), with 2,2'-Bipyridine (bpy) and curcumin (curcu). The complexes were obtained in good yields (92-94%). The structures of complexes were verified by microanalyses and spectroscopic methods. The compositional analyses of complexes indicate 1:1:1 metal, curcumin and 2, 2'-bipyridine stoichiometries. Mass spectrometric analysis of the complexes showed a molecular ion peak [M]⁺, formed by the loss of one chlorine atom from the parent molecule due to the high temperatures employed in the experimental setup.

All three metal complexes revealed their elemental analysis satisfactorily. After decomposition of the complexes the tests for the anions were found to be positive, which exhibited their presence inside the coordination sphere. Curcumin and 2, 2'-bipyridine both behaved as bidentate ligand. Curcumin coordinated to metal by deprotonation of hydroxyl group (enol form) and thus (=) bond becomes resonating between both the oxygen of carbonyl group. The complexes are insoluble in water and/or in non polar organic solvents but found to be soluble in DMSO and

DMF. With the help of analytical, spectroscopic and magnetic data the possible structures of complexes were established.

Conductance

The molar conductivities of the complexes in DMSO (10⁻³ M solutions) were determined at 25 °C. The values 63, 68 and 72 Ω⁻¹ cm² mol⁻¹ for (**1**), (**2**) and (**3**) complexes respectively, indicate that these complexes are 1:1 electrolytes; consequently one chloride ion is present outside the coordination sphere.

Vibrational spectra

From IR spectral data (**Figure 2**) of the complexes (**1-3**), it can be noticed that ν(O-H) band at 3423 cm⁻¹ has disappeared which confirmed the disappearance of hydroxyl group of enol form with the persistence of phenolic group vibrational band (3470-3500 cm⁻¹, O-H stretch, narrow non bonded hydroxyl group and 1340-1415 cm⁻¹ phenol O-H band)²⁵ which strongly suggest its non-involvement in coordination to metal ion²⁶ whereas, O-H absorption (enol form) of free curcumin appeared at 1620 cm⁻¹.²⁷ The carbonyl (>C=O) stretching vibration displayed weak bands at 1610, 1606 and 1595 cm⁻¹ for (**1**), (**2**) and (**3**) complexes respectively, shifting these bands to lower frequency confirm its involvement in coordination.²⁸ Bands observed in the range of 3008-3020 cm⁻¹ may be assigned due to ν(C-H) stretching vibrations of benzene ring.²⁹

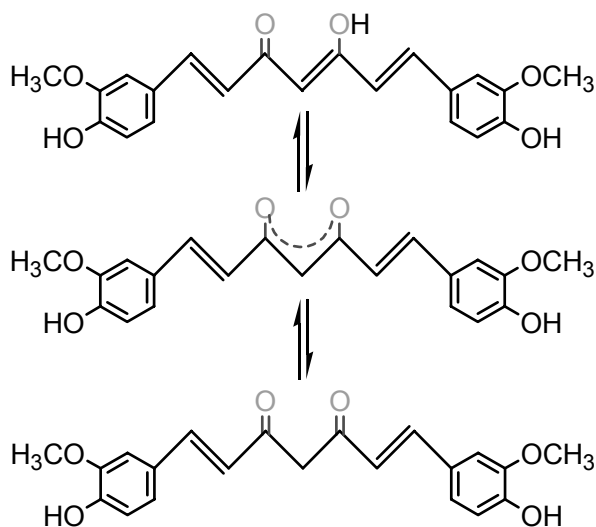


Fig. 1 – Tautomeric forms of curcumin.

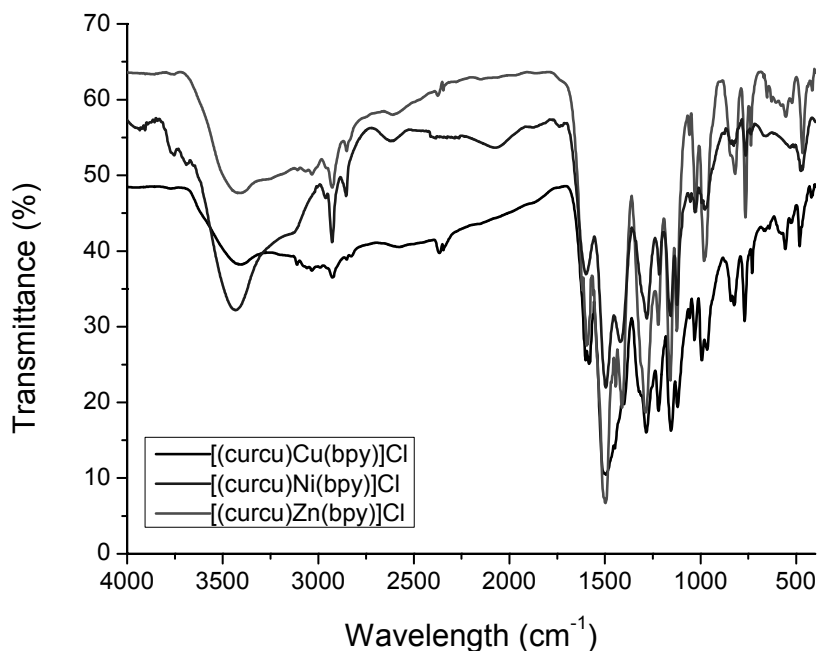


Fig. 2 – Infrared spectra of complexes.

Various absorption bands in the range of 1510–1620 cm^{-1} may be due to $\nu(\text{C}=\text{C})$ aromatic stretching vibrations of benzene ring and aliphatic ($\text{C}=\text{C}$) in curcumin moiety. The value of $\nu(\text{C}=\text{N})$ stretching vibration of 2,2' bipyridine moiety 1590–1625 cm^{-1} is found to be lower than the value of free bpy. This lower shifting in values of $\nu(\text{C}=\text{N})$ stretching may be explained on the basis of a drift of lone pairs density of bpy nitrogen atoms towards the metal ions³⁰⁻³¹ indicating that coordination takes place through bpy nitrogen atoms. Bands in the region of 2950 and 2860 cm^{-1} are assigned to asymmetric and symmetric stretching vibrations of the methyl group, while bands at 1440 and 1375 cm^{-1} further support the presence of asymmetric and symmetric bending mode of methyl group respectively. Bands in far IR region 556–580 cm^{-1} and 440–465 cm^{-1} are assigned to $\nu(\text{M}-\text{N})$ and $\nu(\text{M}-\text{O})$ stretching vibrations respectively.³¹

Magnetic Susceptibility Studies and Electron Spin Resonance Spectra

The magnetic momentum data support the formation of complexes (1), (2) and (3). In case of complex (1), room temperature magnetic susceptibility measurements μ_{eff} was found to be 0.4 B.M. Generally, Ni(II) prefers a low-spin square planar geometry with diamagnetic behavior, while a tetrahedral system has magnetic moment values about to 3.9 B.M., this value varies then the Ni(II) complex prepared in this study (1). Slight paramagnetism in complex (1) can be attributed

due to the existence of a mixture of singlet ($S = 0$) and triplet ($S = 1$) states, because the singlet is the ground state and the triplet is the low-lying excited state of Ni(II) ions. Such type of anomalous magnetic behavior has been observed earlier for square planar Ni(II) complexes.³² The presence of a mixture or an equilibrium between spin-free (triplet state, two unpaired electrons) and spin-paired (singlet state, no unpaired electron), the configuration is not forbidden, especially if the $\text{dx}^2\text{-y}^2$ orbital is not highly destabilized during the change of the ground state from singlet to triplet. Due to closeness of these two levels, there could be a thermal population in both levels, which may result in an intermediate magnetic moment for complex (1).

It is evident that Cu(II) square planar complexes exhibit magnetic moments in the range 1.8–2.1 BM. These values are slightly higher than the spin only value of 1.73 BM and this is due to the spin-orbit coupling followed by lowering of symmetry. The magnetic moment obtained for complex (2) is 1.80 μ_{B} , corresponding to the presence of one unpaired electron, which is characteristic for the square planar geometry and attributed to spin orbit coupling.³³⁻³⁴ The ESR spectrum of the complex (2) was recorded in DMSO at 300 and 77 K, illustrated in **Figure 3(a)** and **3(b)** respectively. The spectrum at 77 K was almost identical to that at room temperature, which indicates that the geometry of Cu(II) did not change after lowering the temperature. The values of $g_{\parallel}^{\text{II}}$ and g_{\perp}^{II} were found to be 2.534 and 2.092; the value of $g_{\parallel}^{\text{II}}$ was higher than that of g_{\perp}^{II} . This suggests that $\text{dx}^2\text{-y}^2$

was ground state of Cu(II) ions, which is characteristic of a square-planar geometry.

Magnetic susceptibility studies indicate diamagnetic nature of complex (3) and it indicates the d^{10} outer electronic configuration of zinc.

Electronic Absorption Spectral Studies

The UV-Vis. spectral bands of the complexes in DMSO solution were measured at room temperature and compared with pure curcumin (Figure 4). Electronic absorption spectrum of the nickel (II) d^8 complex (1), square-planar, consists of four absorption bands, *i.e.* 28089, 23148, 21881, and 18518 cm^{-1} . The lowest energy band lying at 18518 cm^{-1} is assigned to the parity-forbidden

$^1B_{1g} \leftarrow ^1A_g$ transition, and the higher energy band at 21881 cm^{-1} to the $^1B_{3g} \leftarrow ^1A_g$ transition. The shoulder at 23148 cm^{-1} and a strong band at 28089 cm^{-1} are assigned to $d-d$, $^1B_{2u} \leftarrow ^1A_g$ and $^1B_{3u} \leftarrow ^1A_g$ transitions respectively.³⁵

The spectrum of copper (II) complex (2) displays a well-defined shoulder around 21739-22831 cm^{-1} , attributable to $^2A_{1g} \leftarrow ^2B_{1g}$ and $^2B_{2g} \leftarrow ^2B_{1g}$ transitions which strongly favor the square planar geometry around the central metal ion.³⁶⁻³⁷

The broadness of the band may be taken as an indication of distortion from perfect planar symmetry. On the lower energy side, a very weak shoulder at 18148 cm^{-1} may be attributed to the $^2B_{3g} \leftarrow ^2B_{1g}$ $d-d$ transition. Magnetic moment 1.80 BM further supports the proposed geometry.³⁸

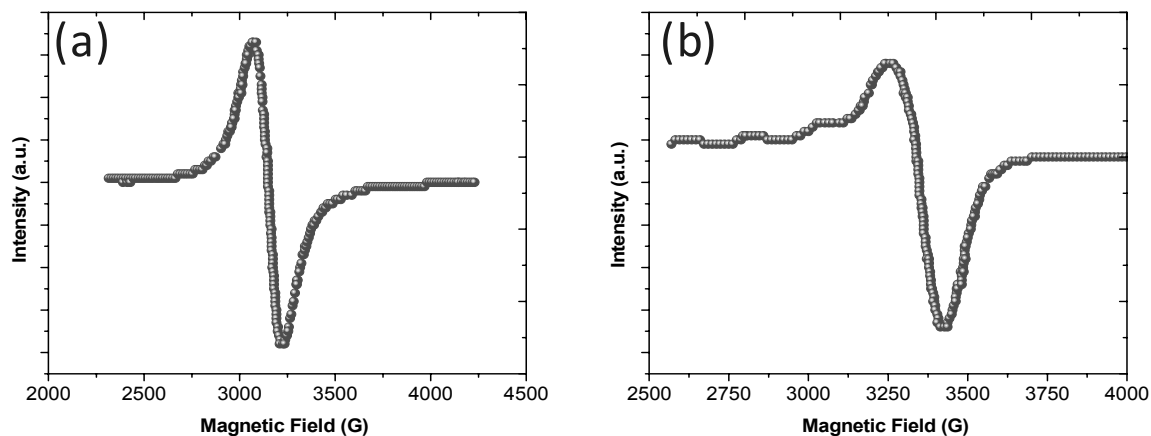


Fig. 3 – ESR spectra of complex (2).

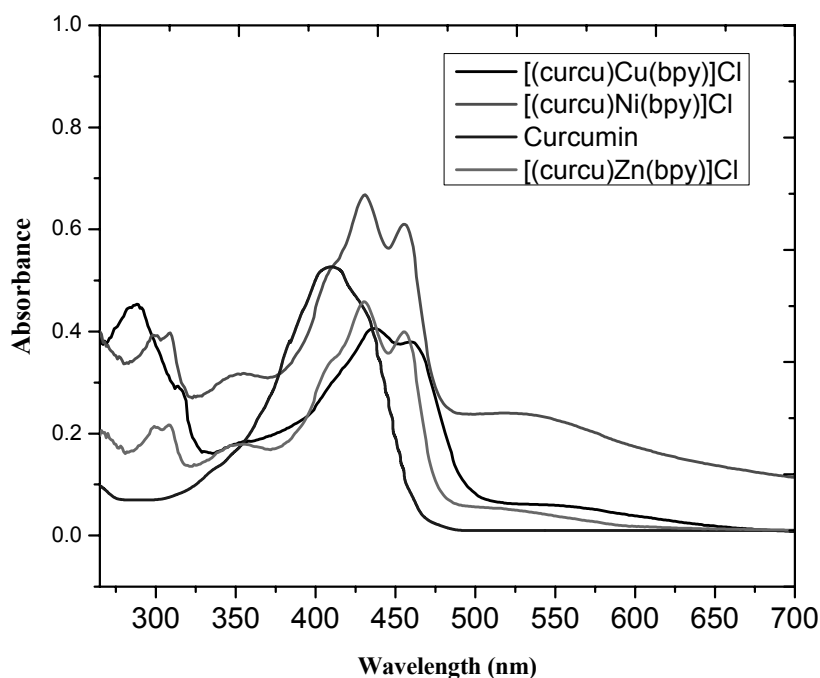
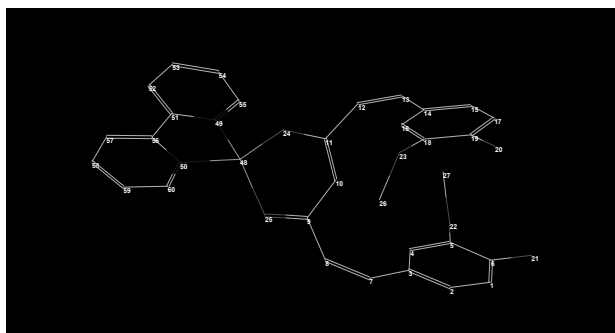
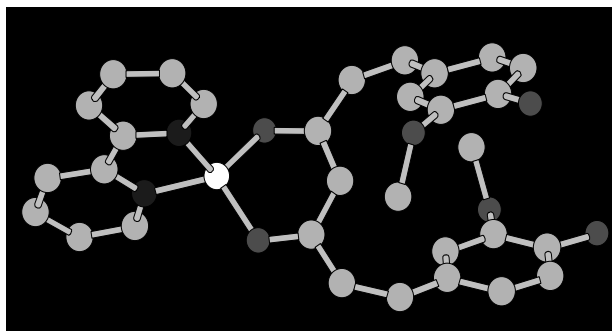


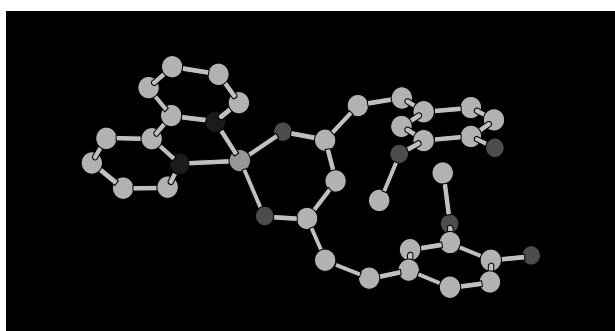
Fig. 4 – Absorption spectra of the complexes (1)-(3) in comparison with curcumin.



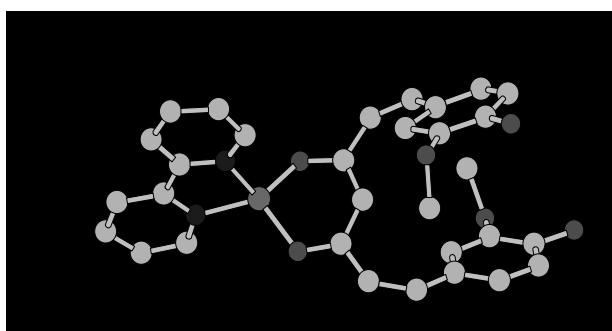
(a) Numbering system in the complexes



(b) [(curcu)Ni(bpy)]Cl



(c) [(curcu)Cu(bpy)]Cl



(d) [(curcu)Zn(bpy)]Cl

Fig. 5 – The energy minimized structure (a) Figure showing numbering in the complexes (b) [(curcu)Ni(bpy)]Cl (c) [(curcu)Cu(bpy)]Cl (d) [(curcu)Zn(bpy)]Cl.

Molecular modeling

Geometry optimization was done by the molecular mechanics method (MM+) for ligands and their metal complexes. Molecular mechanics

attempts to reproduce molecular geometries, energies and other parameters like bond angles and bond lengths. In order to obtain energy values and other structural details of these complexes we have optimized the molecular structure of the

complexes. Energy minimization was repeated several times by constraining different geometries, *i.e.* tetrahedral and square planar to find the global minimum. Their energy minimized structures have been represented in **Figure 5 (a), (b), (c) and (d)**.

These energy-minimized structures were obtained by geometric optimization of the structures using molecular mechanics force field, Mm plus, and the steepest descent algorithm. The cyan colors represent carbon atoms and white, red, blue, green and purple colors represent nickel, oxygen, nitrogen, copper and zinc respectively.

Antimicrobial activity

Curcumin, 2,2' bipyridine and all three metal complexes were evaluated for *in vitro* microbial activity against four bacteria (two Gram positive and two Gram negative) and two fungi. An insight on the data from **Figure 6** exhibit all the compounds that have variable activity against used microbial strains. Though, complexes are less toxic than ligands individuals. Data clearly exhibit that copper complex possess a remarkable antimicrobial activity against most of the pathogens. The following important points may be summarizing:

- 1) i) against *S. aureus* the order of activity of the complexes is Cu > Ni > Zn.
 ii) against *S. epidermidis* the order of activity of the complexes is Ni > Cu > Zn.
 iii) against *E. coli* the order of activity of the complexes is Ni > Cu > Zn.
 iv) against *Klebsiella pneumonia* the order of activity of the complexes is Cu > Ni > Zn.
 v) against *Aspergillus niger* the order of activity of the complexes is Cu > Zn > Ni.
 vi) against *Candida albicans* the order of activity of the complexes is Cu > Ni > Zn.
- 2) The tested compounds are more active against Gram positive bacteria than Gram negative fungi, which is probably related to the structural difference among the bacteria as well as in fungi. Some antibiotics have the capability to inhibit a step in the synthesis of ptidoglycan resulting death of bacteria. Gram positive and Gram negative bacteria have a difference in their cell wall. Gram positive bacteria possess thick cell wall of multiple folds of ptidoglycan and teichoic acids whereas Gram negative bacteria possess a relatively thin cell wall of

few layers ptidoglycan surrounded by lipid membrane containing lipopoly-saccharides and lipoproteins. These cell wall structural differences may be responsible for different antibacterial susceptibility against antibiotics.³⁹

- 3) In our study, the metal complex shows an increased activity than their parent ligand, which may be explained on the basis of Overtones concept and chelation theory.⁴⁰⁻⁴¹ According to Overtone's concept of cell permeability, the lipid membrane that surrounds the cell favors the passage of only lipid-soluble materials due to which liposolubility is an important factor which controls the antimicrobial activity. On chelation, the polarity of the metal ion will be reduced to a greater extent due to the overlap of the ligand orbital and partial sharing of the positive charge of the metal ion with donor groups. Further, it increases the delocalization of π -electrons over the whole chelate ring and enhances the lipophilicity of the complexes. This increased lipophilicity enhances the penetration of the complexes into lipid membranes and blocks the metal binding sites in the enzymes of microorganisms.
- 4) Such work may have significance in designing more active agents for therapeutic purposes through SAR, toxicity and biological effects.

EXPERIMENTAL

Materials and spectral measurements

All chemicals used were Analar or of high grade. The compounds used were purchased from E-Merck, India and used without further purification. Elemental analyses were carried out on Elementar Analysen Systeme GmbH Vario EL-III instrument. Molar conductance of the complexes (**1-3**) (10^{-3} mol L⁻¹) in DMSO were measured at room temperature using a digital conductivity bridge from ELICO. FT-IR spectra (4000-200 cm⁻¹) of some reactants and complexes were recorded from KBr discs using a Perkin-Elmer FTIR-2000 spectrometer. Electronic spectra of the complexes (10^{-3} mol L⁻¹; DMSO) were recorded on Thermo UV-10 UV-VIS spectrophotometer. Analysis of the metal present was determined by the complex decomposition with conc. HNO₃. So obtained solution was diluted with deionised distilled water and then filtered off. EDTA titration was carried out according to the literature⁴²⁻⁴³ Magnetic moments were measured on vibrating sample magnetometer (model 155). ESI-MS mass spectra were obtained from the LC-TOF (KC-455) mass spectrometer of Waters.

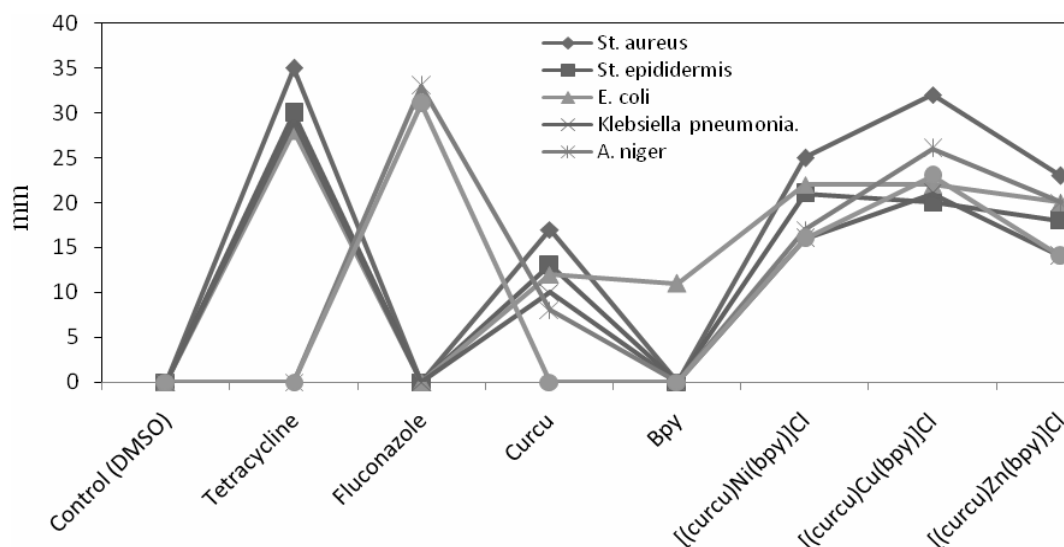


Fig. 6 – The inhibition zone diameter (mm) of curcu, bpy and metal complexes.

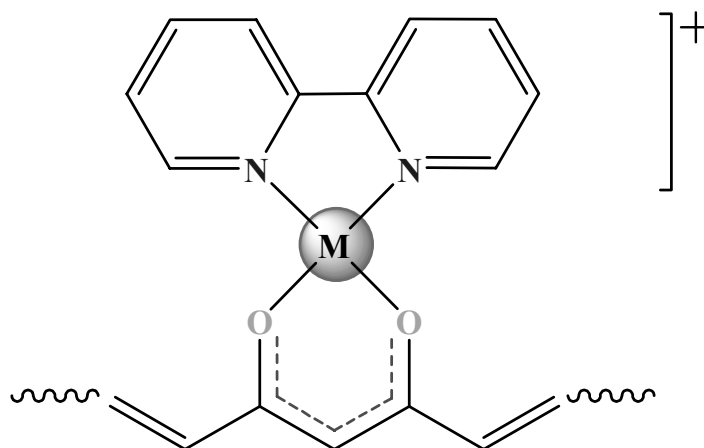


Fig. 7 – Proposed metal complexes, M = Ni^{II}, Cu^{II} and Zn^{II}.

Syntheses of complexes 1–3

Complexes [(curcu)M(bpy)]Cl (M = Ni^{II} (**1**); Cu^{II} (**2**); Zn^{II} (**3**)) were prepared by following a general synthetic procedure with minor changes.⁴⁴ An ethanolic solution (10 mL) of hydrated metal chloride (1mmol) for Cu^{II} (0.1704 g), Ni^{II} (0.2377 g), and Zn^{II} (0.1723 g) was added drop-wise to a CH₂Cl₂ solution (10 mL) of 2,2'-bipyridine (0.1561 g, 1mmol) with stirring for 2 days at 25 °C. The resulting solid was filtered, washed with cold ethanol followed by diethyl ether to obtain [M(bpy)Cl₂] as precursor complex which was dried in vacuum and used in the next step.

To a methanol suspension (10 mL) of the precursor complex [M(bpy)Cl₂] (0.1429 g, Ni^{II}; 0.1453 g, Cu^{II}; 0.1462 g, Zn^{II}), 0.5 mmol was added the curcumin ligand (0.1842 g, 0.5mmol) dissolved in methanol (10 mL) and the pH of the reaction mixture was adjusted to 5-7 by adding aqueous ammonia. The resulting solution was refluxed overnight and then it was allowed to slow evaporation. The corresponding color complexes were precipitated, collected by filtration. Solid thus obtained was washed thoroughly with cold ethanol, distilled water followed by diethyl ether and finally dried in vacuum over CaCl₂ (Figure 7). The characterization data for the complexes are given below.

[(curcu)Ni(bpy)]Cl (1): Molecular Formula (F. Wt.): C₃₁H₂₇NiN₂O₆Cl (617.70). Yield: 92%. Color: Brick red. Anal. Calc.: C, 60.28; H, 4.41; N, 4.54; Ni, 9.50. Found: C, 60.32; H, 4.38; N, 4.50; Ni, 9.58 %. ESI-MS (*m/z*): 581.13 [M]⁺. FT-IR, cm⁻¹: 3480 and 1340 br (Ar-OH), 1610 s (>C=O), 3008 m (Ar-CH), 2950-2856 s (-CH stretch), 580 s (M-N), 444 s (M-O) (br, broad; vs, very strong; s, strong; m, medium; w, weak). UV-visible in DMSO [λ_{max} , cm⁻¹]: 33557, 32573, 28089, 23148, 21881, 18518. Molar conductance (Λ_M) in DMSO at 25° C: 63 Ω^{-1} cm² mol⁻¹.

[(curcu)Cu(bpy)]Cl (2): Molecular Formula (F. Wt.): C₃₁H₂₇CuN₂O₆Cl (622.55). Yield: 94%. Color: Rusty red. Anal. Calc.: C, 49.40; H, 3.84; N, 8.54; Cu, 10.21. Found: C, 49.51; H, 3.95; N, 8.38%; Cu, 10.01. ESI-MS (*m/z*): 586.12 [M]⁺. FT-IR, cm⁻¹: 3500 and 1380 br (Ar-OH), 1606 s (>C=O), 3020 m (Ar-CH), 2945-2860 s (-CH stretch), 572 s (M-N), 440 s (M-O) (vs, very strong; s, strong; m, medium; w, weak). UV-visible in DMF [λ_{max} , cm⁻¹]: 34722, 28490, 22831, 21739, 18148. Molar conductance (Λ_M) in DMSO at 25° C: 68 Ω^{-1} cm² mol⁻¹.

[(curcu)Zn(bpy)]Cl (3): Molecular Formula (F. Wt.): C₃₁H₂₇ZnN₂O₆Cl (624.40). Yield: 93%. Color: Coral red.

Anal. Calc.: C, 49.40; H, 3.84; N, 8.54; Zn, 10.47. Found: C, 49.51; H, 3.95; N, 8.38%; Zn, 10.75. ESI-MS (m/z): 587.12 $[M]^+$. FT-IR, cm^{-1} : 3485 and 1415 br (Ar-OH), 1595 s ($>C=O$), 3012 m (Ar-CH), 2948-2855 s (-CH stretch), 556 s (M-N), 465 s (M-O) (vs, very strong; s, strong; m, medium; w, weak). UV-visible in DMF [λ_{max} , cm^{-1}]: 33557, 32467, 28653, 23255, 21978, 18796. Molar conductance (Λ_M) in DMSO at 25 °C: $72 \Omega^{-1} cm^2 mol^{-1}$.

Solubility and stability

The complexes were soluble in DMF, DMSO; less soluble in MeCN and insoluble in hydrocarbons. They were stable in the solid and solution phases.

Molecular Modeling

Molecular modeling to propose the structure of complexes (**1-3**) was performed using Hyper Chem version 7.51 program package. The correct stereochemistry was assured through the manipulation and modification of the molecular coordinates to obtain reasonable low energy molecular geometries. The potential energy of the molecule was the sum of the following terms (E) = $E_{str} + E_{ang} + E_{tor} + E_{vdw} + E_{oop} + E_{ele}$, where all E 's represent the energy values corresponding to the given types of interaction (kcal/mol). The subscripts str, ang, tor, vdw, oop and ele denote bond stretching, angle bonding, torsion deformation, van der waals interactions, out of plain bending and electronic interaction, respectively. The molecular mechanics describes the application of classical mechanics to the determination of molecular equilibrium structures. It enables the calculation of the total static energy of a molecule in terms of deviations from reference unstrained bond lengths, angles and torsions plus non-bonded interactions. On account of non-bonded interactions and also the chemical sense of each atom, treat the force field as a set of constants that have to be fixed by appeal to experiment or more rigorous calculations. It has been found that off-diagonal terms are usually the largest when neighboring atoms are involved, and so we have to take account of non-bonded interactions, but only between next-nearest neighbors.

Antimicrobial activity

Curcumin and its derivatives have been found to possess wide biological activities.⁴⁵⁻⁴⁶ Thus it becomes logical to explore antimicrobial activities of the synthesized complexes against two Gram positive [*Streptococcus aureus* (MTCC 96), *Streptococcus epidermidis* (MTCC 435)], two Gram negative [*Klebsiella pneumonia* (MTCC 530), *Escherichia coli* (MTCC 443)] bacteria and two fungi [*Aspergillus niger* (MTCC 1344), *Candida albicans* (MTCC 227)] selected on the basis of their clinical importance for commonly causing diseases in humans. A number of pathogens, including *C. albicans*, have evolved mechanisms that attenuate the efficiency of phagosome-mediated inactivation, promoting their survival and replication within the host.⁴⁷ Serious drug-drug interactions toxicity, severe drug resistance and non-optimal pharmacokinetics are striking problems observed in the antifungal therapy.⁴⁸⁻⁴⁹ Because of all these striking problems, there is an immediate need to develop novel antibacterial and antifungal drugs with higher efficiency, broader spectrum, improved pharmacodynamic profiles, and lower toxicity.

To determine the activities of the ligands and synthesized complexes the disc agar diffusion method⁵⁰⁻⁵¹ was employed.

As standards tetracycline and fluconazole were used in case of bacteria and fungi respectively, while DMSO as control. The studied bacteria and fungi were incubated into Nutrient Broth for 24 h and Malt-Extract Broth for 48 h, respectively. In this method, Nutrient agar for bacteria and Malt-Extract agar sterilized in a flask and cooled to 50 °C was distributed (50 mL) to sterilized Petri dishes (15 cm in diameter) after injecting 0.1 mL cultures of bacterium or fungus, prepared as mentioned above and allowed to solidify. Uniform size filter paper discs (3 discs per compound) were impregnated by 10 μ L in concentration of 50 mg/mL of the tested compounds. The Petri dishes were left at 4 °C for 2 h and then the plates were incubated at 30 °C for bacteria (18–24 h) and (72 h) for fungi. At the end of the experiment, inhibition zones formed on the medium were evaluated as millimeters (mm) diameter. Inhibition of the organisms which evidently clear the zone around the paper disc and the values recorded are the mean average.

CONCLUSIONS

Three metal complexes (**1-3**) were synthesized by the reaction of 1,7-Bis(4-hydroxy-3-methoxyphenyl)-1,6-heptadiene-3,5-dione and 2,2'-bipyridine with Ni^{II} , Cu^{II} and Zn^{II} metal ions in very good yields. These chemical entities are encouraging and may serve as new generation of compounds that could be biologically significant and perhaps better than ligands alone employed in the study. Physicochemical and spectral studies revealed that complex (**1**) and (**2**) possess square planar geometry and complex (**3**) favors tetrahedral. The examined complexes show significant differences for their antimicrobial activities in comparison with the corresponding free ligands. Complex (**2**) exhibited overall excellent inhibition against the employed pathogens.

Acknowledgements. Authors give thanks to the Principal, A. N. D. College (DU) for providing laboratory facilities. V. K. also thanks "Department of Biotechnology (DBT)" for support of this research (Grant No. BT/PR13120/GBD/27/188/2009).

REFERENCES

1. T. H. Cooper, G. Clark and J. Guzinski, in C.-T. Ho (Ed.), "Food Phytochemicals II, Teas, Spices and Herbs", American Chemical Society, Washington, DC, 1994, p. 231–236.
2. A. J. Ruby, G. Kuttan, K. D. Babu, K. N. Rajasekharan and R. Kuttan, *Cancer Lett.*, **1995**, *94*, 79–83.
3. K. M. Nelson, J. L. Dahlin, J. Bisson, J. Graham, G. F. Pauli, and M. A. Walters, *J. Med. Chem.*, **2017**, *60*, 1620–1637.
4. F. Yan, J. L. Sun, W. H. Xie, L. Shen and H. F. Ji, *Nutrients*, **2018**, *10*, 28, 1–11.
5. M. Salem, S. Rohani and E. R. Gillies, *RSC Adv.*, **2014**, *4*, 10815–10829.

6. J. Adiwidjaja, A. J. McLachlan and A. V. Boddy, *Expert Opin. Drug Metab. Toxicol.*, **2017**, 953-972.
7. E. Ferrari, R. Benassi, S. Sacchi, F. Pignedoli, M. Asti, M. Saladini, *J. Inorg. Biochem.*, **2014**, 139, 38-48.
8. R. S. Moamen, *Spectrochim. Acta Part A—Mol. Biomol. Spectrosc.*, **2013**, 105, 326-337.
9. M. Prohl, U. S. Schubert, W. Weigand, M. Gottschaldt, *Coord. Chem. Rev.*, **2016**, 307, 32-41.
10. F. Ahmadi, A. A. Alizadeh, N. Shahabadi and M. Rahimi-Nasrabadi, *Spectrochim. Acta Part A—Mol. Biomol. Spectrosc.*, **2011**, 79, 1466-1474.
11. S. Banerjee and A. R. Chakravarty, *Acc. Chem. Res.*, **2015**, 48, 2075–2083.
12. S. Wanninger, V. Lorenz, A. Subhan and F. T. Edelmann, *Chem. Soc. Rev.*, **2015**, 44, 4986-5002.
13. I. Shlar, E. Poverenov, Y. Vinokur, B. Horev, S. Droby and V. Rodov, *Nano-Micro Lett.*, **2015**, 7, 68-79.
14. J. Chen, Z. MinHe, F. Wang, Z. Zhang, X. Liu, D. Zhai and W. Chen, *E. J. Pharm.*, **2016**, 772, 33-42.
15. M. Asti, E. Ferrari, S. Croci, G. Atti, S. Rubagotti, M. Iori, P.C. Capponi, A. Zerbin, M. Saladini and A. Versari, *Inorg. Chem.*, **2014**, 53, 922-4933.
16. Y. Sunagawa, Y. Katanasaka, K. Hasegawa and T. Morimoto, *Pharma Nut.*, **2015**, 3, 131-135.
17. P. Malik and M. Singh, *New J. Chem.*, **2017**, 41, 12506-12519.
18. V. Kumar, T. Ahamad and N. Nishat, *Eur. J. Med. Chem.*, **2009**, 44, 785-793.
19. J. Markham, J. Liang, A. Levina, R. Mak, B. Johannessen, P. Kappen, C. J. Glover, B. Lai, S. Vogt and P. A. Lay, *Eur. J. Inorg. Chem.*, **2017**, 1812–1823.
20. A. Zahirovic, E. Kahrovic, M. Cindric, S. K. Pavelic, M. Hukic, A. Harej and E. Turkusic, *J. Coord. Chem.*, **2017**, 70, 4030-4053.
21. A. Wojciechowska, A. Gagor, M. Duczmal, Z. Staszak and A. Ozarowski, *Inorg. Chem.*, **2013**, 52, 4360–4371.
22. W. Liu, X. Chen, Q. Ye, Y. Xu, C. Xie, M. Xie, Q. Chang and L. Lou, *Inorg. Chem.*, **2011**, 50, 5324-5326.
23. B. S. Murray, S. Crot, S. Siankevich and P. J. Dyson, *Inorg. Chem.*, **2014**, 53, 9315-9321.
24. K. Krishnankutty and P. Venugopal, *Synth. React. Inorg. Met. Org. Chem.*, **1998**, 28, 1313-1325.
25. D. Pucci, A. Crispini, B. S. Mendiguchia, S. Pirillo, M. Ghedini, S. Morellib and L. D. Bartolob, *Dalton Trans.*, **2013**, 42, 9679-9687.
26. M. I. Khalil, A. M. Al-Zahem and M. H. Al-Qunaibit, *Bioinorg. Chem. & Appl.*, Article ID 982423 2013, pages 5.
27. D. Pucci, T. Bellini, A. Crispini, I. D'Agnano, P. F. Liguori, P. Garcia-Orduna, S. Pirillo, A. Valentinid and G. Zanchettab, *Med. Chem. Commun.*, **2012**, 3, 462-468.
28. A. Barik, B. Mishra, L. Shen, H. Mohan, R. M. Kadam, S. Dutta, H.-Y. Zhang and K. I. Priyadarsini, *Free Radic. Biol Med.*, **2005**, 39, 811-822.
29. D. P. Singh, R. Kumar, V. Malik and P. Tyagi, *Trans. Met. Chem.*, **2007**, 32, 1051-1055.
30. M. A. Satish, M. P. Sathisha and V. K. Revankar, *Trans. Met. Chem.*, **2007**, 32, 81-87.
31. K. Nakamoto, "Infrared and Raman spectroscopy of Inorganic and Coordination Compounds", 4th edition, Wiley, New York, 1986.
32. E. Simon-Manso, M. Valderrama and D. Boys, *Inorg. Chem.*, **2001**, 40, 3647-3649.
33. A. P. Zambre, V. M. Kulkarni, S. Padhye, S. K. Sandurc and B. B. Aggarwal, *Bio. Med. Chem.*, **2006**, 14, 7196-7204.
34. N. Nishat, M. M. Haq, T. Ahamad and V. Kumar, *J. Coord. Chem.*, **2007**, 60, 85-96.
35. B. N. Figgis, "Introduction to Ligand Fields", John Wiley/Interscience Publishers, Inc., New York, 1966.
36. A. B. P. Lever, "Inorganic Electronic Spectroscopy", 2nd edition, Elsevier, New York, 1968.
37. F. A. Cotton and G. Wilkinson, "Advanced Inorganic Chemistry", 5th edition, Wiley, New York, 1988.
38. V. Kumar, T. Ahamad and N. Nishat, *J. Coord. Chem.*, **2008**, 61, 1036-1045.
39. A. L. Koch, *Clin. Microbiol. Rev.*, **2003**, 16, 673-687.
40. Y. Anjaneyula and R. P. Rao, *Synth. React. Inorg. Met. Org. Chem.*, **1986**, 16, 257-272.
41. R. Malhotra, S. Kumar and K. S. Dhindsa, *Indian J. Chem.*, **1993**, 32A, 457-459.
42. A. I. Vogel, "Textbook of quantitative inorganic analysis", 4th edition, Longman Press, London, 1978.
43. H. A. Flaschka, "EDTA titration", 2nd edition, Pergamon Press, Oxford, 1964.
44. D. Pucci, A. Crispini, B. S. Mendiguchia, S. Pirillo, M. Ghedini, S. Morellib and L. D. Bartolob, *Dalton Trans.*, **2013**, 42, 9679-9687.
45. G. O'Sullivan-Coyne, G. C. O'Sullivan, T. R. O'Donovan, K. Piwocka and S. L. McKenna, *British J. Cancer*, **2009**, 101, 1585-1595.
46. B. Chhunchha, N. Fatma, B. Bhargavan, E. Kubo, A. Kumar and D. P. Singh, *Cell Death & Disease*, **2011**, 2, e234.
47. J. M. Bain, J. Louw, L. E. Lewis, B. Okai, C. A. Walls, E. R. Ballou, L. A. Walker, D. Reid, C. A. Munro, A. J. P. Brown, G. D. Brown, N. A. R. Gow and L. P. Erwig, *mBio.*, **2014**, 5, e01874-14.
48. S. Vilar, E. Uriarte, L. Santana, T. Lorberbaum, G. Hripcsak, C. Friedman and N. P. Tatonetti, *Nature Protocols*, **2014**, 9, 2147-2163.
49. C. A. Rabik and M. E. Dolan, *Cancer Treat. Rev.*, **2007**, 33, 9-23.
50. A. W. Bauer, W. M. Kirby, J. C. Sherris and M. Turck, *Am. J. Clinical Path.*, **1966**, 45, 493-496.
51. A. Alagumaruthanayagam, A. R. Pavankumar, T. K. Vasanthamallika and K. Sankaran, *The J. Antibiotics*, **2009**, 62, 377-384.

